mRNAs and miRNAs in whole blood associated with lung hyperplasia, fibrosis, and bronchiolo-alveolar adenoma and adenocarcinoma following multi-walled carbon nanotube inhalation exposure in mice

Brandi N. Snyder-Talkington[1], **Chunlin Dong**[2], **Linda M. Sargent**[1], **Dale W. Porter**[1], **Lauren M. Staska**[3], **Ann F. Hubbs**[1], **Rebecca Raese**[2], **Walter McKinney**[1], **Bean T. Chen**[1], **Lori Battelli**[1], **David T. Lowry**[1], **Steven H. Reynolds**[1], **Vincent Castranova**[4], **Yong Qian**[1,*], and **Nancy L. Guo**[2,*]

[1]Pathology and Physiology Research Branch, Health Effects Laboratory Division, National Institute for Occupational Safety and Health, Morgantown, WV 26505, USA

[2]Mary Babb Randolph Cancer Center, West Virginia University, Morgantown, WV 26506-9300, USA

[3]WIL Research, Hillsborough, NC 27278, USA

[4]Department of Basic Pharmaceutical Sciences, School of Pharmacy, West Virginia University, Morgantown, WV 26506, USA

Abstract

Inhalation exposure to multi-walled carbon nanotubes (MWCNT) in mice results in inflammation, fibrosis, and the promotion of lung adenocarcinoma; however, the molecular basis behind these pathologies is unknown. This study determined global mRNA and miRNA profiles in whole blood from mice exposed by inhalation to MWCNT that correlated with the presence of lung hyperplasia, fibrosis, and bronchiolo-alveolar adenoma and adenocarcinoma. Six-week-old, male, B6C3F1 mice received a single intraperitoneal injection of either the DNA-damaging agent

*Corresponding Authors Yong Qian, Pathology and Physiology Research Branch, Health Effects Laboratory Division, National Institute for Occupational Safety and Health, 1095 Willowdale Road, Morgantown, WV 26505-2888, Tel: +1 304 285 6286; Fax: +1 304 285 5938; yaq2@cdc.gov. Nancy L. Guo, Mary Babb Randolph Cancer Center and Department of Community Medicine, West Virginia University, Morgantown, WV 26506-9300, USA. Telephone: +1 304 293 6455; Fax: +1 304 293 4667; lguo@hsc.wvu.edu. BNT – ifp1@cdc.gov. CD – cdong@hsc.wvu.edu. LMSargent – lqs1@cdc.gov. DWP – dhp7@cdc.gov. LMStaska – lauren.staska@wilresearch.com. AFH – afh0@cdc.gov. RR – raraese@gmail.com. WM – wdm9@cdc.gov. BTC – bdc4@cdc.gov. LB – lob0@cdc.gov. DTL – dhl5@cdc.gov. SHR – sir6@cdc.gov. VC – vcastran@hsc.wvu.edu. YQ – yaq2@cdc.gov. NLG – lguo@hsc.wvu.edu.

Disclaimer

The findings and conclusions in this report are those of the author(s) and do not necessarily represent the views of the National Institute for Occupational Safety and Health. Mention of a brand name does not constitute product endorsement.

Competing Interests

The authors declare that they have no competing interests.

methylcholanthrene (MCA, 10 µg/g body weight) or vehicle (corn oil). One week after injections, mice were exposed by inhalation to MWCNT (5 mg/m³, 5 hours/day, 5 days/week) or filtered air (control) for a total of 15 days. At 17 months post-exposure, mice were euthanized and examined for the development of pathological changes in the lung, and whole blood was collected and analyzed using microarray analysis for global mRNA and miRNA expression. Numerous mRNAs and miRNAs in the blood were significantly up- or down-regulated in animals developing pathological changes in the lung after MCA/corn oil administration followed by MWCNT/air inhalation, including *fcrl5* and miR-122-5p in the presence of hyperplasia, *mthfd2* and miR-206-3p in the presence of fibrosis, *fam178a* and miR-130a-3p in the presence of bronchiolo-alveolar adenoma, and *il7r* and miR-210-3p in the presence of bronchiolo-alveolar adenocarcinoma, among others. The changes in miRNA and mRNA expression, and their respective regulatory networks, identified in this study may potentially serve as blood biomarkers for MWCNT-induced lung pathological changes.

Keywords

mRNA; miRNA; MWCNT; MCA; fibrosis; adenocarcinoma

Introduction

Multi-walled carbon nanotubes (MWCNT) are concentric cylinders of graphene that have numerous physicochemical properties, making them ideal for industrial and electronic applications (Ajayan, 1999; Iijima, 1991). The small aerodynamic diameter of MWCNT may allow for easy aerosolization; therefore, potential exposure during MWCNT production, use, and disposal is a concern (Castranova, 2011). Inhaled MWCNT can reach the conducting airways of the lung and enter the alveolar region, and MWCNT have been repeatedly shown to be bioactive within cells *in vitro* and induce inflammation and fibrosis *in vivo* (Mercer, *et al.*, 2013a; Mercer, *et al.*, 2013b; Porter, *et al.*, 2013; Porter, *et al.*, 2010; Snyder-Talkington, *et al.*, 2013b; Snyder-Talkington, *et al.*, 2013c). While some MWCNT are cleared from the lung by macrophages , a fraction of deposited MWCNT can translocate into the pleural cavity or distribute systemically, potentially following macrophage engulfment (Mercer, *et al.*, 2013b). The majority of MWCNT remain in the alveolar region for a year or more post-exposure, where they can elicit a pathological response.

Inflammation of the lung epithelium is a common effect of MWCNT exposure both *in vivo* and *in vitro* (Mercer, *et al.*, 2013a; Porter, *et al.*, 2013; Porter, *et al.*, 2010; Snyder-Talkington, *et al.*, 2013b). *In vivo*, increases in lactate dehydrogenase, albumin levels, and polymorphonuclear leukocytes in the bronchoalveolar lavage fluid of mice exposed to MWCNT by both aspiration and inhalation are indicative of an inflammatory response (Mercer, *et al.*, 2013a; Porter, *et al.*, 2013; Porter, *et al.*, 2010), while changes in inflammatory gene signatures and inflammasome activation indicate an inflammatory response *in vitro* (Hussain, *et al.*, 2014; Snyder-Talkington, *et al.*, 2013b). Injury of the alveolar-capillary barrier and the associated inflammatory response typically resolve with time post-exposure; however, repetitive injury can result in a dysregulated response, loss of alveolar integrity and structure, inappropriate establishment of extracellular matrix, and the

promotion of pulmonary fibrosis (Strieter, 2008). Pulmonary fibrosis has a poor clinical outcome (Ley, *et al.*, 2011) and has been associated with an increased risk of lung cancer (Lee, *et al.*, 2014; Vancheri, *et al.*, 2010), with the majority of cancers being found in areas of prior lung fibrosis (Lee, *et al.*, 2014). Although a direct connection between human MWCNT inhalation exposure and cancer has yet to be determined, the known effects of MWCNT (oxidative stress, genotoxicity, inflammation, and fibrosis) can be pathobiologically linked to tumor promotion and cancer progression (Donaldson, *et al.*, 2012; Pitot, 1993). MWCNT have been shown to interact with mitotic spindles and disrupt mitosis, potentially through incorporation of the MWCNT into microtubules, resulting in aberrant separation of chromosomes during cell division (Siegrist, *et al.*, 2014). Additionally, MWCNT inhalation exposure following the administration of a DNA-damaging agent, methylcholanthrene (MCA), promoted the growth and neoplastic progression of lung adenocarcinoma in B6C3F1 mice (Sargent, *et al.*, 2014). The etiology and path of progression from MWCNT exposure to pathological conditions is unknown; however, biomarkers to detect pulmonary changes before they reach an end-stage disease state are actively being sought (Ley, *et al.*, 2014).

We have previously shown that genome-wide mRNA expression in mouse lungs exposed by aspiration to MWCNT could stratify human lung cancer patients into good and poor prognosis groups (Guo, *et al.*, 2012). Additionally, circulating mRNAs and miRNAs in blood are potentially attractive for studies of individuals with lung disease as objective markers of lung pathological changes (Bremnes, *et al.*, 2005). In this study, we determined significant up- or down-regulation of blood mRNA and miRNA expression in mice after MWCNT inhalation exposure that correlated with the presence of lung inflammation, fibrosis, or bronchiolo-alveolar adenoma or adenocarcinoma. These changes may be associated with the onset and progression of MWCNT-induced lung pathology and potentially serve as biomarkers for lung disease following exposure.

Materials and Methods

MWCNT

The MWCNT used in this study were obtained from Hodogaya Chemical Company (MWCNT-7, lot #061220-31) and have been previously described (Sargent, *et al.*, 2014). Briefly, the MWCNT were manufactured using a floating reactant catalytic chemical vapor deposition method, followed by high temperature thermal treatment in argon at 2500°C using a continuous furnace as previously described (Kim, *et al.*, 2005). The bulk material was characterized by a high-resolution transmission electron microscopy (TEM) under a Philips CM 20 TEM with an EDS (EDAX/4p1) as previously described (McKinney, *et al.*, 2009). MWCNT trace metal contamination was 1.32%, with iron being the major trace metal contaminant (1.06%) (Porter, *et al.*, 2013).

MWCNT Inhalation Exposure

The animal study described here has been previously published (Sargent, *et al.*, 2014). All animals in this study were housed in an AAALAC-accredited, specific pathogen-free, and environmentally controlled facility. All animal studies and procedures were approved by the

National Institute for Occupational Safety and Health ACUC. Six week old, male B6C3F1 (Jackson Laboratories; Bar Harbor, ME) mice were housed singly in polycarbonate ventilated cages with HEPA-filtered air and fed ad libitum with Harlan 7913 irradiated NIH-31 modified 6% rodent chow. After a 1 week acclimation period, mice (60/group) were randomly assigned to each of the exposure groups and treated following a 2-stage, initiation-promotion protocol (Malkinson, *et al.*, 1997). The 2-stage protocol involved the administration of 10 μg/g vehicle (corn oil) or MCA. One week after vehicle or MCA administration, mice were exposed to MWCNT or filtered air by whole body inhalation for 15 days (5 mg/m^3, 5 hours/day, 5 days/week). Details of the MWCNT aerosol were previously described (Sargent, *et al.*, 2014). Animals were monitored weekly, and those with overt signs of morbidity or changes in body weight were euthanized prior to terminal sacrifice. Mice were euthanized 17 months after exposure to allow time for tumor development (Figure 1).

There were four exposure groups in this study:

(1) Animals receiving a corn oil injection followed by filtered air inhalation exposure (Air).

(2) Animals receiving an MCA injection followed by filtered air inhalation exposure (MCA).

(3) Animals receiving a corn oil injection followed by MWCNT inhalation exposure (MWCNT).

(4) Animals receiving an MCA injection followed by MWCNT inhalation exposure (MCA+MWCNT).

Whole blood collection and RNA isolation

Mice were euthanized with an overdose of 100 mg/kg of pentobarbital, and deep anesthesia was confirmed when the mouse no longer responded to a toe pinch. Approximately 200–400 μL of whole blood was collected from the abdominal aorta, immediately inverted 10 times in a 2 mL tube containing 1 mL of RNAlater, and placed on ice. Following blood collection, the abdominal aorta was transected to provide exsanguination. RNAlater blood samples were stored at -20°C until use.

Total RNA was isolated from mouse blood samples using a Mouse RiboPure™-Blood RNA Isolation Kit from Ambion (Grand Island, NY) according to the manufacturer's protocol. Frozen samples were allowed to thaw at room temperature and centrifuged for 3 min at 12,000 rpm. The supernatant was removed, and the blood pellet was lysed in 1 mL of Lysis Solution. The lysed sample was poured into a 15 mL tube and mixed with 200 μL of 3 M sodium acetate. Lysis Solution was added to produce a total volume of 3.8 mL, and the sample was vortexed for 5 sec. A total of 1.5 mL of acid-phenol:chloroform was added to the lysate, and the tube was shaken vigorously for 30 sec and allowed to sit at room temperature for 5 min. The sample was centrifuged for 10 min at 3200 rpm, and the aqueous phase was recovered into a fresh 15 mL tube. A total of 0.6 volume of nuclease-free water was added to the aqueous phase, the solution was vortexed for 5 sec, and 1.2 volume of ethanol was added and vortexed for 10 sec. Approximately 700 μL of sample was applied to

a filter cartridge and centrifuged for at least 10 sec at 8000 × g to pass the liquid through the filter. The flowthrough was discarded, and the process was repeated until the entire sample had been passed through the filter. The filter was washed once with 750 μL of Wash Solution 1 and twice with 750 μL Wash Solution 2/3, centrifuging for 10 sec between each wash before centrifuging for 1 min at maximum speed to remove residual fluid from the filter. The filter was transferred to a collection tube, and 250 μL of preheated (80°C) Elution Solution was used to elute the total RNA by centrifuging at maximum speed for 1 min.

RNA concentrations were determined using a NanoDrop 1000 Spectrophotometer (NanoDrop Technologies; Wilmington, DE), and RNA quality was assessed using an Agilent 2100 Bioanalyzer (Agilent Technologies; Santa Clara, CA).

mRNA and miRNA microarray profiling

Global mRNA expression profiles were generated with Mouse Gene ST 2.1 plates at the University of Michigan Microarray Facility using an Affymetrix Plus kit. cDNA was synthesized from 500 ng of total RNA, amplified, fragmented, and biotinylated using a GeneChip WT PLUS Reagent kit (Affymetrix; Santa Clara, CA) according to manufacturer's instructions. cDNA was then prepared for hybridization with reagents from the Affymetrix GeneTitan Hybridization, Wash, and Stain Kit for WT Array Plates. For hybridization, 2.76 μg of labeled cDNA were hybridized to the Affymetrix Mouse Gene ST 2.1 Arrays, which were then washed, stained, and scanned using the GeneTitan Multi-Channel Instrument according to Affymetrix's User Guide for Expression Array Plates (P/N 702933 Rev. 2, 2013). Data were analyzed using the Limma, Oligo, and Affy Bioconductor packages implemented in the R statistical environment. The Robust Multi-array Average was used to normalize the data and fit $\log_2$ transformed expression values. The raw microarray data were processed using a robust multi-array average method (Irizarry, *et al.*, 2003), and expression values were $\log_2$ transformed, with a principal component analysis used as the final quality control step to visualize the mRNA expression values. The analysis was performed with the *oligo* package of Bioconductor in the R statistical environment.

For miRNA profiling, RNA samples were sent to Ocean Ridge Biosciences (Palm Beach Gardens, FL) for analysis using custom, multi-species microarrays containing 1,280 mouse miRNA probes present in miRBase version 19. The sensitivity of the microarray is such that it could detect as low as 20 attomoles of synthetic miRNA being hybridized along with each sample. The microarrays were produced by Microarrays Inc. (Huntsville, Alabama) and consisted of epoxide glass substrates that had been spotted in triplicate with each probe. Quality control of the total RNA samples was assessed using UV spectrophotometry and agarose gel electrophoresis. The samples were DNAse digested, and low-molecular weight (LMW) RNA was isolated by ultrafiltration through YM-100 columns (Millipore) and subsequently purified using an RNeasy MinElute Clean-Up Kit (Qiagen; Valencia, CA). The LMW RNA samples were 3'-end labeled with Oyster-550 fluorescent dye using a Flash Taq RNA Labeling Kit (Genisphere; Hatfield, PA). Labeled LMW RNA samples were hybridized to the miRNA microarrays according to conditions recommended in the Flash Taq RNA Labeling Kit manual. The microarrays were scanned on an Axon Genepix 4000B scanner, and data were extracted from images using GenePix V4.1 software.

Microarray data will be submitted to the NIH Gene Expression Omnibus database upon publication.

Lung pathological examination

The pathology methods described here have been previously published (Sargent, *et al.*, 2014). Following euthanasia, lungs were fixed by intratracheal perfusion with 1 mL of 10% neutral buffered formalin. Lungs and any lesions were trimmed the same day and processed overnight. Tissues were embedded in paraffin and sectioned at approximately 5 μm. Hematoxylin and eosin stained slides were prepared for each of the 5 separate lung lobes and from masses identified during necropsy.

Slides were examined by a board-certified veterinary pathologist using light microscopy or polarized light, which was occasionally used to confirm the presence or absence of foreign material. The severity of non-neoplastic lesions was graded on a 4-point scale of minimal (1), mild (2), moderate (3), or marked (4). All lung slides from 10% of the mice were randomly selected for peer review by a second board-certified veterinary pathologist who independently evaluated the slides while blinded to the interpretation of the study pathologist. Pathology categories included normal tissue, focal alveolar hyperplasia, bronchiolo-alveolar hyperplasia, alveolar fibrosis, bronchiolo-alveolar adenoma, and bronchiolo-alveolar adenocarcinoma (Sargent, *et al.*, 2014).

Statistical analysis of changes in mRNA and miRNA expression associated with lung pathological changes

mRNA data were analyzed using Statistical Analysis System (SAS) version 9.3 to perform an ANOVA test with the Benjamini and Hochberg (B-H) adjustment method. An mRNA was considered statistically significant if the p-value was <0.05 with a 10% FDR and FC >1.5.

Two methods were used for miRNA data analyses: (1) Significance Analysis of Microarrays (SAM) was used to compare each miRNA in each treatment group and the control group without considering different pathological outcomes. A change in miRNA expression was considered statistically significant at 10% FDR and FC >1.2. The *siggenes* package in the R statistical environment was used for the SAM analysis. (2) An ANOVA test adjusted with the B-H method was used to compare miRNA expression changes between different pathological outcomes in different exposure groups. A change in miRNA expression was considered statistically significant if the p-value was <0.05 with a 10% FDR and fold change >1.5. SAS version 9.3 was used for the ANOVA analysis.

Ingenuity Pathway Analysis (IPA)

IPA was used to determine associations of changes in mRNAs and miRNAs with pathological outcomes, including idiopathic pulmonary fibrosis, inflammation of respiratory system, fibrosis of lung, lung cancer, and non-small cell lung adenocarcinoma. Molecules are represented as nodes, and the biological relationship between two nodes is represented as an edge (line). All edges are supported by at least one reference from the literature, from a textbook, or from canonical information stored in the Ingenuity Knowledge Base. Human,

mouse, and rat orthologs of a gene are stored as separate objects in the Ingenuity Knowledge Base but are represented as a single node in the network. Nodes are displayed using various shapes that represent the functional class of the gene product. To create connections between significant mRNAs and miRNAs and pathology outcomes, the Grow – Diseases and Functions tool of IPA was used.

Results

Overall pathological changes

Mice were exposed in a 2-stage protocol involving the administration of 10 μg/g vehicle (corn oil) or MCA. One week after vehicle or MCA administration, mice were exposed to MWCNT or filtered air by whole body inhalation for 15 days (5 mg/m^3, 5 hours/day, 5 days/ week). Animals were monitored weekly, and those with overt signs of morbidity or changes in body weight were euthanized prior to terminal sacrifice. Mice were euthanized 17 months after exposure to allow time for tumor development (Figure 1). The lungs of all animals were examined microscopically, and the following lesions were identified: focal alveolar hyperplasia, fibrosis, bronchiolo-alveolar hyperplasia, lymphohistiocytic inflammation, bronchiolo-alveolar adenoma, and bronchiolo-alveolar adenocarcinoma. Focal alveolar hyperplasia was defined by increased cellularity in a discrete, random location and was composed of crowded alveolar epithelial cells outlining contiguous alveolar septa. Bronchiolo-alveolar hyperplasia was a multifocal lesion seen as increased numbers of cuboidal or polygonal aciliate epithelial cells lining the terminal bronchioles, alveolar ducts, and/or adjacent alveoli. For all further analyses, both focal alveolar hyperplasia and bronchio-alveolar hyperplasia are referred to together as "hyperplasia". Fibrosis was seen as increased amounts of collagen which thickened the interstitium, and lymphohistiocytic inflammation was characterized by increased numbers of lymphocytes and macrophages in alveolar spaces or expanding the interstitium. Bronchiolo-alveolar adenomas were focal and expansile masses composed of polygonal and uniform cells that distorted and replaced the alveolar architecture and obliterated alveolar spaces. Cells typically formed irregular papillary structures, ribbons, or solid clusters separated by delicate, fibrovascular stroma. In contrast, bronchiolo-alveolar adenocarcinomas had increased cellular atypia, higher nuclear to cytoplasm ratios, and prominent nucleoli. Bronchiolo-alveolar adenocarcinomas also contained several patterns, including ribbons, papillary structures, or solid clusters. The numbers of mice falling into each pathology category are listed in Table 1.

Whole blood was analyzed for total mRNA and miRNA expression, and the numbers of blood samples for mRNA and miRNA analyzed in each pathology category are listed in Table 1. If a mouse harbored more than one type of lung pathology, that mouse was counted into each respective pathology category.

Blood mRNA and miRNA expression in mice with spontaneous induction of lung pathological changes

Of mice in the Air exposure group (those receiving corn oil administration and exposed to filtered air), 23% presented with lung pathological changes (pathology control animals) when compared to Air mice that had no lung pathological changes (normal control animals).

Fourteen percent of pathology control animals had hyperplasia, 2% had fibrosis, and 10% and 12% had bronchiolo-alveolar adenoma and bronchiolo-alveolar adenocarcinoma, respectively (Table 1). Several known and putative mRNAs, as well as multiple miRNAs, were found to be significantly up- or down-regulated in the blood of Air mice with lung pathology (pathology control animals) as compared to the blood of Air mice with no lung pathology (normal control animals) (Table 2). mRNAs and miRNAs found to be altered in pathology control mice (Table 2) are referred to in further analyses as "genetic factors", as these mRNAs and miRNAs may be involved in the formation of lung pathological changes regardless of MCA administration or MWCNT exposure.

Blood mRNA and miRNA expression in mice injected with either MCA or corn oil followed by exposure to air or MWCNT compared with normal control animals

Whole blood mRNA and miRNA expression from MCA, MWCNT, and MCA+MWCNT mice was compared to that of normal control animals (Air mice with no lung pathological changes) to identify mRNAs and miRNAs that may play a role in MCA-induced and MWCNT-induced pathological changes (Table 3).

In the MCA exposure group, 5 (*iqcg, 17202511, siglich, 9830166K06Rik, 1720663*), 8 (17209629, 17210565, olfr1062, gm5512, c1, ceacam19, uck2, 17203041), 13 (17210565, scgb2b26, hpca14, vmn1r65, cd3d, 17257054, serpina3f, d10jhu81e, zcchc9, sptssa, fabp4, scai, fam178a), and 8 (elov13, hpgd, 17202937, akr1c12, ear2, 17460573, fmo3, sp140) known and putative mRNAs were significantly up- or down-regulated when compared to normal control animals in the hyperplasia, fibrosis, bronchiolo-alveolar adenoma, and bronchiolo-alveolar adenocarcinoma pathology categories, respectively, while 6 (miR-29b-3p, miR-15a-3p, miR-362-3p, miR-5112, miR-5131, miR-2137), 5 (miR-5131, miR-2137, miR-466c-5p, miR-6238, miR32-3p), and 7 (miR-345-5p, miR-497-5p, miR-130a-3p, miR-15a-3p, miR-5131, miR-2137, miR-669c-3p) miRNAs were significantly up- or down-regulated in the hyperplasia, fibrosis, and bronchiolo-alveolar adenoma pathology categories, respectively. There were no significant miRNAs in the MCA bronchiolo-alveolar adenocarcinoma category. One miRNA, miR-345-5p in the bronchiolo-alveolar adenoma category, was considered to be a genetic factor.

In the MWCNT exposure group, 6 (17210565, igkv4-91, fcrl5, 17202925, efemp1, gm13139), 2 (*pdgfrb, smad7*), 5 (*A630077, j23Rik, mul6b, ighg3, 17202925*), and 6 (*foxo1, 17210589, fcrl5, fcrla, gpr183, 17202023*) known and putative mRNAs were significantly up- or down-regulated compared to normal control mice in the hyperplasia, fibrosis, bronchiolo-alveolar adenoma, and bronchiolo-alveolar adenocarcinoma pathology categories, respectively, while 2 (miR-122-5p, miR-497-5p), 14 (miR-324-5p, miR-27a, miR-27b-3p, let-7d-3p, miR-30c-1-3p, miR-3072-5p, miR-5107-5p, miR-341-3p, miR-1892, miR-6370, miR-6368, miR-1249-5p, miR-504-3p, miR-1947-3p), and 1 (miR-122-5p) miRNAs were significantly altered in the hyperplasia, fibrosis, and bronchiolo-alveolar adenoma pathology categories, respectively. There were no significant miRNAs in the MWCNT bronchiolo-alveolar adenocarcinoma category. One miRNA, miR-27b-3p in the MWCNT fibrosis category, was considered to be a potential genetic factor.

In the MCA+MWCNT exposure group, 6 (*gpr114, olfr982, 17205523, sloc1a4, il18r1, gm6793*), 5 (*myh7, mthfd2, cd96, tnfrsf23, igh-vj559*), 6 (*17200621, smok2a, krt6a, 17205967, gm6793, fabp4*), and 10 (17207465, c1qbp, il7r, fcrl15, gpr114, prdm9, sap30bp, krt6a, 17200649, 17202925) known and putative mRNAs and 3 (miR-5112, miR-345-5p, miR-1957), 12 (miR-101b-3p, miR-29c-3p, miR-340-5p, miR-19b-5p, miR-672-5p, miR-574-5p, miR-206-3p, miR-6348, miR-32-3p, miR-466o-5p, miR-466c-5p, miR-669k-5p), 13 (miR-345-5p, miR-144-3p, miR-122-5p, miR-19a-3p, miR-29b-3p, miR-19b-3p, miR-5112, miR-5131, miR-15a-3p, miR-466c-5p, miR-5099, miR-5121, miR-1957), and 6 (miR-5112, miR-5131, miR-210-3p, miR-19b-3p, miR-345-5p, miR-466c-5p) miRNAs were significantly up- or down-regulated when compared to normal control mice in the hyperplasia, fibrosis, bronchiolo-alveolar adenoma, and bronchiolo-alveolar adenocarcinoma pathology categories, respectively. One miRNA in the MCA +MWCNT fibrosis category, miR-29c-3p; 6 miRNAs in the MCA+MWCNT bronchiolo-alveolar adenoma category, miR-345-5p, miR-144-3p, miR-29b-3p, miR-19b-3p, miR-5112, and miR-466c-5p; and 2 miRNAs in the MCA+MWCNT bronchiolo-alveolar adenocarcinoma category, miR-19b-3p and miR-345-5p, were considered to be possible genetic factors. In the significantly up- and down-regulated mRNAs, a few mRNAs were shared between disease groups. *Fcrl5* was significantly down-regulated in the MWCNT hyperplasia, MWCNT bronchiolo-alveolar adenocarcinoma, and the MCA+MWCNT bronchiolo-alveolar adenocarcinoma pathology groups. *Fabp4* was significantly down-regulated in the MCA bronchiolo-alveolar adenoma and MCA+MWCNT bronchiolo-alveolar adenoma groups, while *krt6a* was significantly upregulated in the MCA+MWCNT bronchiolo-alveolar adenoma group but down-regulated in the MCA+MWCNT bronchiolo-alveolar adenocarcinoma group.

With regard to the miRNAs, several miRNAs were significantly up- or down-regulated across multiple pathology groups. MiR-5112 was significantly upregulated in the MCA hyperplasia, MCA+MWCNT hyperplasia, MCA+MWCNT bronchiolo-alveolar adenoma, and MCA+MWCNT bronchiolo-alveolar adenocarcinoma groups. MiR-5131 was significantly upregulated in the MCA hyperplasia, MCA fibrosis, MCA bronchiolo-alveolar adenoma, MCA+MWCNT bronchiolo-alveolar adenoma, and MCA+MWCNT bronchiolo-alveolar adenocarcinoma groups. MiR-2137 was significantly upregulated in the MCA hyperplasia, MCA fibrosis, and MCA bronchiolo-alveolar adenoma groups. MiR-497-5p was significantly upregulated in the MCA bronchiolo-alveolar adenoma and MWCNT hyperplasia groups, while miR-466c-5p was significantly upregulated in the MCA fibrosis but down-regulated in the MCA+MWCNT fibrosis, MCA+MWCNT bronchiolo-alveolar adenoma, and MCA+MWCNT bronchiolo-alveolar adenocarcinoma groups.

Regulatory networks involving significant mRNAs and miRNAs

To determine regulatory networks involving significantly up- or down-regulated mRNAs and miRNAs in each category, all significant mRNAs and miRNAs observed in each exposure and pathology category were analyzed using an IPA miRNA target filter. All significantly altered miRNAs in each category were input into IPA and matched against only those mRNAs that were also significantly altered in the same category. Interaction networks were found in three exposure groups within at least one of their pathology categories. The

MCA bronchiolo-alveolar adenoma category included predicted mRNA/miRNA relationships between miR-130a-3p/fam178a and miR-497-5p/scai/hpcal4 (Figure 2A). The MWCNT-induced hyperplasia category included a predicted mRNA/miRNA relationship between miR-122-5p and fcrl5 (Figure 2B). The MCA+MWCNT fibrosis category included an experimentally validated mRNA/miRNA relationship between miR-206-3p and mthfd2 (Selbach, *et al.*, 2008) and a predicted mRNA/miRNA relationship between miR-574-5p and cd96 (Figure 2C).

Association of significant mRNAs and miRNAs with literature-based pathological outcomes

IPA analysis was also used to determine significant mRNAs and miRNAs in the blood of all exposure groups that were identified in the literature (IPA Knowledge Base®) to be associated with lung diseases, including the IPA disease and functions idiopathic pulmonary fibrosis, inflammation of respiratory system, fibrosis of lung, lung cancer, and non-small cell lung adenocarcinoma (Figure 3). Five mRNAs and miRNAs, *pdgfrb* (FDA, 2013), miR-18b-5p (Pandit, *et al.*, 2010), miR-19b-3p (Pandit, *et al.*, 2010), miR-29b-3p (Pandit, *et al.*, 2010; Pandit, *et al.*, 2011), and miR-27a (Oak, *et al.*, 2011), were associated with "idiopathic pulmonary fibrosis"; six mRNAs and miRNAs, *smad7* (Hanada, *et al.*, 2002), *pdgrfb* (FDA, 2013), miR-18b-5p (Pandit, *et al.*, 2010), miR-19b-3p (Pandit, *et al.*, 2010), miR-29b-3p (Pandit, *et al.*, 2010; Pandit, *et al.*, 2011), and miR-27a (Oak, *et al.*, 2011), were associated with "inflammation of respiratory system"; six mRNAs and miRNAs, *pdgfrb* (FDA, 2013), *smad7* (Gressner, *et al.*, 2002; Nakao, *et al.*, 1999), miR-27a (Oak, *et al.*, 2011), miR-29b-3p (Pandit, *et al.*, 2010; Pandit, *et al.*, 2011), miR-18b-5p (Pandit, *et al.*, 2010), and miR-19b-3p (Pandit, *et al.*, 2010), were associated with "fibrosis of lung"; ten mRNAs and miRNAs, *hpgd* (NCI, 2007), *pdgfrb* (FDA, 2008), *il7r* (COSMIC, 2014a), *krt6b* (Imielinski, *et al.*, 2012; Savci-Heijink, *et al.*, 2009), *scai* (COSMIC, 2014b), miR-497-5p (Bandi, *et al.*, 2009), miR-18b-5p (Hwang, *et al.*, 2007), miR-19b-3p (Garofalo, *et al.*, 2011; Hwang, *et al.*, 2007), miR-27b-3p (Wang, *et al.*, 2011), and miR-210-3p (Puissegur, *et al.*, 2011; Raponi, *et al.*, 2009; Redova, *et al.*, 2011; Seike, *et al.*, 2009), were associated with "lung cancer"; and three mRNAs and miRNAs, *scai* (COSMIC, 2014b), *krt6b* (COSMIC, 2014a), and miR-497-5p (Bandi, *et al.*, 2009), were associated with "non-small cell lung adenocarcinoma".

To determine potential mRNA and miRNA regulatory networks involving the mRNAs and miRNAs associated with known pathological outcomes (Figure 3), the Build-Connect function of IPA was used to determine predicted and known interactions. Interactions of miR-29b-3p with *pdgfrb* and *scai*, miR-27b-3p with *scai*, miR-18b-5p with *pdgfrb*, and miR-497-5p with *scai* and *smad7* are predicted to occur by the TargetScan database. An interaction between *smad7* and miR-29b-3p (Liu, *et al.*, 2013) was found in the IPA Knowledge Base.

Blood mRNA and miRNA expression in mice with bronchiolo-alveolar adenocarcinoma versus bronchiolo-alveolar adenoma in each exposure group

In addition to determining those mRNAs and miRNAs in the blood that are potentially related to the effects of MCA administration or MWCNT exposure, we evaluated mRNA

and miRNA responses in each exposure category that were significantly altered between mice presenting with bronchiolo-alveolar adenoma and adenocarcinoma to identify potential regulators of the transition from adenoma to adenocarcinoma (Table 4). In the Air and MCA groups, 26 mRNAs and 6 miRNAs and 40 mRNAs and 11 miRNAs, respectively, were significantly up- or down-regulated in mice presenting with adenocarcinoma versus mice presenting with adenoma (Table 4). In the MWCNT and MCA+MWCNT groups, 23 mRNAs and 7 miRNAs and 40 mRNAs and 6 miRNAs, respectively, were significantly up- or down-regulated in mice presenting with adenocarcinoma versus mice presenting with adenoma (Table 4).

To determine potential signaling networks involving mRNAs and miRNAs in bronchiolo-alveolar adenocarcinoma compared to adenoma, significantly changed miRNAs (false discovery rate [FDR] <10%, fold change [FC] >1.5) were matched against only those significantly changed mRNAs) FDR <10%, FC >1.5) in the same exposure group using an IPA miRNA target filter. Direct and indirect mRNA associations were found in the Air group between *stat3* and *gas6* (Yanagita, *et al.*, 2001), *kras* (Kang, *et al.*, 2012), and *adm* (Dauer, *et al.*, 2005) and between *ednrb* and *adm* (Dschietzig, *et al.*, 2007), with predicted mRNA and miRNA regulatory relationships between miR-130a-3p and *stat3* and *birc6* (Figure 4A). In the MCA group, direct and indirect mRNA associations were found between *ddx17* and *mll5* (Zhou, *et al.*, 2013), *spib* and *bcl6* (Wei, *et al.*, 2009), *bcl6* and *il7r* (Sawant, *et al.*, 2012), and *il7r* and *cd5* (Tani-ichi, *et al.*, 2013) (Figure 4B). A predicted mRNA and miRNA relationship was found between miR-130a-3p and *mdfy4* (Figure 4B). In the MCA +MWCNT group, there were no relationships between any of the miRNAs and mRNAs, but there were direct and indirect mRNA associations found between *stat3* and *gm13288* (Oritani, *et al.*, 2000), *socs2* (Posselt, *et al.*, 2011), *cdh5* (Mohri, *et al.*, 2006), *il6st* (Junk, *et al.*, 2014), *mpl* (Piu, *et al.*, 2002), and *kdr* (Korpelainen, *et al.*, 1999), and between *kdr* and *cdh5* (Nawroth, *et al.*, 2002), *vwf* (Xiong, *et al.*, 2009), and *pf4* (Jouan, *et al.*, 1999) (Figure 4C). There were no relationships found between the significant mRNAs and miRNAs in the MWCNT exposure group.

To determine signaling pathways involving the significant mRNAs and miRNAs between bronchiolo-alveolar adenoma and adenocarcinoma, IPA dataset analysis was run on the significantly up- and down-regulated mRNAs and miRNAs in each treatment group. In the Air group, the top 5 canonical pathways associated with the up- and down-regulated mRNAs and miRNAs were oncostatin-M signaling, regulation of the epithelial-mesenchymal transition pathway, CNTF signaling, Erb2-Erb3 signaling, and thrombopoietin signaling. The top 5 canonical pathways associated with the up- and down-regulated mRNAs and miRNAs in the MCA group were Gα signaling, regulation of eIF4a and p70S6K signaling, B cell receptor signaling, cAMP-mediated signaling, and colorectal cancer metastasis signaling. The top 5 canonical pathways associated with the up- and down-regulated mRNAs and miRNAs in the MWCNT group were dermatan sulfate degradation (metazoa), polyamine regulation in colon cancer, role of lipids/lipid rafts in the pathogenesis of influenza, thyroid cancer signaling, and unfolded protein response. The top 5 canonical pathways associated with the up- and down-regulated mRNAs and miRNAs in the MCA+MWCNT group were D-glucuronate degradation I, acute phase response

signaling, STAT3 pathway, agranulocyte adhesion and diapedesis, and methylglyoxal degradation III.

Discussion

Markers of disease states, particularly respiratory diseases, are eagerly being sought as measures of disease development and progression (Wu, *et al.*, 2014). The ability to monitor the development of MWCNT-induced pathological changes is essential when attempting to determine the effects of MWCNT in the lung and the progression to lung disease (Ley, *et al.*, 2014). In this study, we used microarray technology to determine global mRNA and miRNA expression and identified numerous significantly up- or down-regulated mRNAs and miRNAs in the blood of mice with normal lungs or those presenting with pathological lung changes induced by administration of MCA or corn oil, followed by inhalation exposure to MWCNT or filtered air. There is a growing discussion concerning the use of experimental animals in toxicological research and the desire to reduce, refine, and replace *in vivo* studies with high-throughput *in vitro* techniques (Marone, *et al.*, 2014; Russell, 1995). Our group has recently shown that an *in vitro* coculture of human small airway epithelial cells and human microvascular endothelial cells following MWCNT exposure produced more concordant gene expression with *in vivo* mouse lungs exposed by aspiration to MWCNT than either cell type in monoculture (Snyder-Talkington, *et al.*, 2015; Snyder-Talkington, *et al.*, 2013c). Although these advanced coculture methods are useful tools for high-throughput screening of toxicity pathways associated with nanomaterial exposure that are more reflective of the *in vivo* environment, long-term animal exposures are still necessary to determine mRNA and miRNA changes that are reflective of progressive pathological states that cannot be achieved *in vitro*. These changes in miRNA and mRNAs expression and their respective regulatory networks may potentially serve as blood biomarkers for MWCNT-induced lung pathological changes.

There is currently extensive interest in investigating pulmonary disease-related miRNAs and their associated mRNAs for use as markers of disease presence and progression. The Encyclopedia of DNA Elements Project estimates that approximately 62% of all DNA is transcribed into RNA elements, which can be divided into protein-coding mRNAs and non-coding short, long, and housekeeping RNAs (Booton, *et al.*, 2014; Dunham, *et al.*, 2012). The regulatory relationship between miRNA and mRNA has been heavily studied since its discovery (Lee, *et al.*, 1993), and transcriptomic analysis of miRNA and mRNA expression profiles in disease states is promising for the determination of disease-related regulatory networks (Ferte, *et al.*, 2013). miRNAs are small, approximately 22-nucleotide non-coding RNAs that regulate mRNA expression by binding complementary sequences in the 3' UTR region of a target mRNA, marking the mRNA for degradation or translational repression (Beezhold, *et al.*, 2010). Regulation of this essential miRNA/mRNA expression balance is imperative for the maintenance of homeostasis, and changes in this balance may be responsible for the onset of disease states in the lung (Booton, *et al.*, 2014).

As exposures to nanoparticles and nanomaterials, particularly MWCNT, result in pulmonary inflammation, fibrosis, tumor promotion, and cancer progression, inhalation of particles during their synthesis, use, and disposal are significant concerns in the growing

nanotechnology field (Mercer, *et al.*, 2013a; Porter, *et al.*, 2013; Sargent, *et al.*, 2014). We have previously identified mRNA profiles in mouse lung tissues exposed by aspiration to MWCNT that could stratify human lung cancer patients into low- and high-risk populations (Guo, *et al.*, 2012). Additionally, we have identified system-based mRNA pathways associated with toxicity in these samples that correlated with the presence of MWCNT-induced inflammation and fibrosis (Porter, *et al.*, 2010; Snyder-Talkington, *et al.*, 2013a). Genes identified by this novel computational method were confirmed *in vitro* to be concordant with *in vivo* expression, suggesting that computational analysis of gene expression can be used to identify molecules and interaction networks giving rise to lung disease (Snyder-Talkington, *et al.*, 2013a). While our previous studies of pathology-related interaction networks involved mRNA and miRNA analysis of lung tissue following MWCNT aspiration exposure (Dymacek, *et al.*, 2014; Snyder-Talkington, *et al.*, 2013a), this current study determined mRNA and miRNA in blood samples from mice exposed by inhalation to MWCNT.

Biomarkers found in blood as compared to tissue allow for less-invasive measurements that can be taken at shorter intervals with lower costs (Ganepola, *et al.*, 2014). While miRNAs are more stable in biological fluids and less prone to degradation due to their short length, determination of both miRNA and mRNA blood expression may allow for downstream analysis of mRNA and miRNA interaction networks that may be more specific for certain pathological conditions. The presence of biomarkers in blood and plasma has been associated with the presence of pathological conditions in the lung, and their presence has been suggested as a way to detect and monitor lung disease (Carolan, *et al.*, 2014; Redova, *et al.*, 2013; Schaaij-Visser, *et al.*, 2013).

In this study, we identified mRNAs and miRNAs in the blood of mice with lung inflammation, fibrosis, or bronchiolo-alveolar adenoma or adenocarcinoma that were either significantly up- or down-regulated as compared to mice with normal lung tissue. The mouse strain used in this study, male B6C3F1 mice, has a lung adenoma background of 2–30% (Sargent, *et al.*, 2014) independent of MCA administration or MWCNT inhalation exposure. To detect miRNA and mRNA alterations due to spontaneous disease, we compared mRNAs and miRNAs in mice in the Air group that developed lung pathological changes (pathology control mice) as compared to Air mice that had normal lung tissue (normal control mice). These were termed "genetic factors", and we suggest that these are involved in the development of a particular abnormality regardless of MCA administration or MWCNT inhalation exposure.

The identification of significantly altered mRNAs and miRNAs in the MCA, MWCNT, and MCA+MWCNT groups allowed us to identify mRNA and miRNA expression in blood that could be specific to MCA administration, MWCNT exposure, or the administration of MCA followed by exposure to MWCNT. MWCNT may potentially act as a carcinogen; or, they may promote tumorigenesis in the presence of an initiator (Nagai, *et al.*, 2011; Rittinghausen, *et al.*, 2014; Sargent, *et al.*, 2014). In this study, MCA, a DNA damaging agent, was used as an initiator in the carcinogenic process (Sargent, *et al.*, 2014). However, the ability of MWCNT alone to significantly alter specific mRNAs and miRNAs in the blood of MWCNT-exposed mice suggests that they have the ability to induce pathological

changes in the lung. In the MCA+MWCNT group, the number of significantly altered mRNA and miRNA increased dramatically. This may be due to exacerbation of each process after both MCA administration and MWCNT exposure. As humans are routinely exposed to chemicals in the air, the potential for inhalation exposure to an initiator is high. Therefore, it is relevant that MWCNT exposure be studied in the presence of a DNA-damaging agent.

There were a few mRNAs and miRNAs that were commonly up- or down-regulated across exposure groups. Three mRNAs, *fcrl5, fapb4,* and *krt6a,* were found in numerous exposure groups and are involved in B-cell differentiation, lipid transport, and epithelial tissue structure, respectively. Although there is little information currently available on the roles of specific miRNAs, miR-5112 and miR-2137 play a role in B-cell development, while miR-497-5p and miR-466c-5p are suggested to play a role in atherosclerosis and motorneuron degeneration, respectively. The ability to determine regulatory networks between significant mRNAs and miRNAs in each individual pathology category (Figure 2) gives a brief view of signaling that may be present under that condition; however, lung pathological changes follow a progression. Therefore, identifying mRNA and miRNA signaling networks that may be involved in numerous outcomes (Figure 3) may provide insight into signaling networks over the course of lung disease progression. Both sets of regulatory networks are useful in attempting to determine potential biomarkers of pathologic signaling following MCA administration and/or MWCNT inhalation exposure. By using the IPA Ingenuity Knowledge Base®, we were able to determine if any of our identified mRNAs and miRNAs were previously associated with a particular lung pathology, particularly pulmonary hyperplasia, fibrosis, adenoma, or adenocarcinoma. Of the five IPA pathologies highlighted in our analysis (idiopathic pulmonary fibrosis, fibrosis of lung, inflammation of respiratory system, lung cancer, and non-small cell lung adenocarcinoma) one genetic factor, miR-19b-3p, was shared between four of the pathologies, suggesting a role as an early and ubiquitous player in the development of lung disease. MiR-19b-3p is a member of the miR-17-92 cluster, a cluster of six miRNAs on human chromosome 13q31 in a region that is frequently amplified in lung cancer (Garofalo, *et al.*, 2011). Upregulation of this region has been associated with increased cell proliferation (Hayashita, *et al.*, 2005), and, in our study, miR-19b-3p was up-regulated in mice presenting with bronchiolo-alveolar adenoma and adenocarcinoma in the MCA+MWCNT exposure group. This finding further suggests that miR-19b-3p may be a potential blood marker for the presence of lung disease. As miR-18b-5p, miR-29b-3p, miR-27a, and *pdgfrb* were also involved in a majority of the five categories, their ubiquitous involvement may suggest an early role in the development of lung disease.

We also determined significantly altered mRNA and miRNA expression between mice presenting with bronchiolo-alveolar adenoma and adenocarcinoma. Bronchiolo-alveolar adenoma is most often characterized by slow-growing, low-malignancy tumors and follows the progression from hyperplasia to adenoma to adenocarcinoma (Pandiri, 2014). Little is known about the molecular mechanisms behind the switch from relatively low-risk abnormalities into high-risk adenocarcinoma, and the potency of MWCNT to induce either pathological state is also unknown. Although there were numerous direct and indirect

interactions between up- and down-regulated mRNAs and their respective protein products, a few predicted mRNA and miRNA regulatory networks were found. As the mechanism behind the switch from adenoma to adenocarcinoma is relatively unknown, elucidation of any mRNA or miRNA involved in this process, regardless of their potential regulations, is beneficial to understanding the disease progression.

By determining the top five canonical pathways associated with the mRNAs and miRNAs significant to bronchiolo-alveolar adenocarcinoma as compared to adenoma, we may be able to determine activated pathways that are crucial to the transition from adenoma to adenocarcinoma. The top five canonical pathways associated with the Air pathology group are involved in the initiation and progression of inflammation, loss of epithelial features with mesenchymal transition, neuronal cell survival after injury, cell growth and transformation, and hematopoiesis, respectively. As the mice that developed adenocarcinoma in this control group received no MCA administration or MWCNT exposure, these signaling pathways may be inherent to the progression of adenoma to adenocarcinoma. The top five canonical pathways associated with the MCA group are involved in chemokine signal transduction, protein translation, B-cell development, and cancer progression. As mice in this group received MCA administration but were not exposed to MWCNT, these pathways may represent the effects of the DNA-damaging initiator on the progression to lung adenocarcinoma. The top five canonical pathways associated with the MWCNT group are involved in wound repair, fibrosis, and tumorigenesis; cell growth, proliferation, and invasion; and cell apoptosis due to stress to the endoplasmic reticulum. Tumor invasion has been shown to be associated with centrosome disruption and rapidly evolving errors in chromosome number (D'Assoro, *et al.*, 2002; Lingle, *et al.*, 2002; Pitot, 1993). As MWCNT *in vitro* have been shown to be bioactive and have effects on centrosome fragmentation, disruption of the cell cycle, and errors in chromosome number (Siegrist, *et al.*, 2014), these pathways may be reflective of the cytotoxic and aneugenic effects of MWCNT. The top five canonical pathways associated with the MCA+MWCNT group are involved in lipid metabolism and glycolysis; the inflammatory response; cell proliferation, invasion, and tumor immune evasion; and leukocyte migration. The dual impact of DNA damage by both MCA administration followed by MWCNT exposure may initiate synergistic signaling pathways that enhance inflammation and tumor progression.

The ability to detect miRNA and mRNA markers for the presence and progression of lung disease in a readily available form, in this case, whole blood, allows for minimally invasive collection, and monitoring can be repeated as necessary. In this study, we chose to not only evaluate significantly up- or down-regulated mRNAs and miRNAs that were involved in lung inflammation, fibrosis, bronchiolo-alveolar adenoma, and adenocarcinoma as compared to normal lung tissue, but we also determined significantly up- or down-regulated mRNAs and miRNAs that may play a role in the progression of benign adenoma to aggressive adenocarcinoma. Limitations of this study include the use of whole blood for the miRNA and mRNAs analysis, as well as no RT-PCR or western blot validation of predicted miRNA and mRNA targets. However, with these matched mRNA and miRNA regulatory networks, it may be possible to predict the onset of lung abnormalities following inhalation exposure

to MWCNT in a minimally invasive manner that may provide early detection and allow treatment before substantial disease progression has occurred.

Acknowledgements

List of Abbreviations

MWCNT	multi-walled carbon nanotubes
MCA	methylcholanthrene
Air group	Mice receiving corn oil injection followed by filtered air exposure
MCA group	Mice receiving MCA injection followed by filtered air exposure
MWCNT group	Mice receiving corn oil injection followed by MWCNT exposure
MCA+MWCNT group	Mice receiving MCA injection followed by MWCNT exposure

References

Ajayan PM. Nanotubes from carbon. Chem Rev. 1999; 99:1787–1800. [PubMed: 11849010]

Bandi N, Zbinden S, Gugger M, Arnold M, Kocher V, Hasan L, Kappeler A, Brunner T, Vassella E. miR-15a and miR-16 are implicated in cell cycle regulation in a Rb-dependent manner and are frequently deleted or down-regulated in non-small cell lung cancer. Cancer Res. 2009; 69:5553–5559. [PubMed: 19549910]

Beezhold KJ, Castranova V, Chen F. Microprocessor of microRNAs: regulation and potential for therapeutic intervention. Mol Cancer. 2010; 9:134. [PubMed: 20515486]

Booton R, Lindsay MA. Emerging role of MicroRNAs and long noncoding RNAs in respiratory disease. Chest. 2014; 146:193–204. [PubMed: 25010962]

Bremnes RM, Sirera R, Camps C. Circulating tumour-derived DNA and RNA markers in blood: a tool for early detection, diagnostics, and follow-up? Lung Cancer. 2005; 49:1–12. [PubMed: 15949585]

Carolan BJ, Hughes G, Morrow J, Hersh CP, O'Neal WK, Rennard S, Pillai SG, Belloni P, Cockayne DA, Comellas AP, Han M, Zemans RL, Kechris K, Bowler RP. The association of plasma biomarkers with computed tomography-assessed emphysema phenotypes. Respir Res. 2014; 15:127. [PubMed: 25306249]

Castranova V. Overview of current toxicological knowledge of engineered nanoparticles. J Occup Environ Med. 2011; 53:S14–17. [PubMed: 21606847]

D'Assoro AB, Barrett SL, Folk C, Negron VC, Boeneman K, Busby R, Whitehead C, Stivala F, Lingle WL, Salisbury JL. Amplified centrosomes in breast cancer: a potential indicator of tumor aggressiveness. Breast Cancer Res Treat. 2002; 75:25–34. [PubMed: 12500932]

Dauer DJ, Ferraro B, Song L, Yu B, Mora L, Buettner R, Enkemann S, Jove R, Haura EB. Stat3 regulates genes common to both wound healing and cancer. Oncogene. 2005; 24:3397–3408. [PubMed: 15735721]

Donaldson K, Poland CA. Inhaled nanoparticles and lung cancer - what we can learn from conventional particle toxicology. Swiss Med Wkly. 2012; 142:w13547. [PubMed: 22714122]

Dschietzig T, Richter C, Asswad L, Baumann G, Stangl K. Hypoxic induction of receptor activity-modifying protein 2 alters regulation of pulmonary endothelin-1 by adrenomedullin: induction

under normoxia versus inhibition under hypoxia. J Pharmacol Exp Ther. 2007; 321:409–419. [PubMed: 17251392]

Dunham I, Kundaje A, Aldred SF, Collins PJ, Davis C, Doyle F, Epstein CB, Frietze S, Harrow J, Kaul R, Khatun J, Lajoie BR, Landt SG, Lee BK, Pauli F, Rosenbloom KR, Sabo P, Safi A, Sanyal A, Shoresh N, Simon JM, Song L, Trinklein ND, Altshuler RC, Birney E, Brown JB, Cheng C, Djebali S, Dong XJ, Dunham I, Ernst J, Furey TS, Gerstein M, Giardine B, Greven M, Hardison RC, Harris RS, Herrero J, Hoffman MM, Iyer S, Kellis M, Khatun J, Kheradpour P, Kundaje A, Lassmann T, Li QH, Lin X, Marinov GK, Merkel A, Mortazavi A, Parker SCJ, Reddy TE, Rozowsky J, Schlesinger F, Thurman RE, Wang J, Ward LD, Whitfield TW, Wilder SP, Wu W, Xi HLS, Yip KY, Zhuang JL, Bernstein BE, Birney E, Dunham I, Green ED, Gunter C, Snyder M, Pazin MJ, Lowdon RF, Dillon LAL, Adams LB, Kelly CJ, Zhang J, Wexler JR, Green ED, Good PJ, Feingold EA, Bernstein BE, Birney E, Crawford GE, Dekker J, Elnitski L, Farnham PJ, Gerstein M, Giddings MC, Gingeras TR, Green ED, Guigo R, Hardison RC, Hubbard TJ, Kellis M, Kent WJ, Lieb JD, Margulies EH, Myers RM, Snyder M, Stamatoyannopoulos JA, Tenenbaum SA, Weng ZP, White KP, Wold B, Khatun J, Yu Y, Wrobel J, Risk BA, Gunawardena HP, Kuiper HC, Maier CW, Xie L, Chen X, Giddings MC, Bernstein BE, Epstein CB, Shoresh N, Ernst J, Kheradpour P, Mikkelsen TS, Gillespie S, Goren A, Ram O, Zhang XL, Wang L, Issner R, Coyne MJ, Durham T, Ku M, Truong T, Ward LD, Altshuler RC, Eaton ML, Kellis M, Djebali S, Davis CA, Merkel A, Dobin A, Lassmann T, Mortazavi A, Tanzer A, Lagarde J, Lin W, Schlesinger F, Xue CH, Marinov GK, Khatun J, Williams BA, Zaleski C, Rozowsky J, Roeder M, Kokocinski F, Abdelhamid RF, Alioto T, Antoshechkin I, Baer MT, Batut P, Bell I, Bell K, Chakrabortty S, Chen X, Chrast J, Curado J, Derrien T, Drenkow J, Dumais E, Dumais J, Duttagupta R, Fastuca M, Fejes-Toth K, Ferreira P, Foissac S, Fullwood MJ, Gao H, Gonzalez D, Gordon A, Gunawardena HP, Howald C, Jha S, Johnson R, Kapranov P, King B, Kingswood C, Li GL, Luo OJ, Park E, Preall JB, Presaud K, Ribeca P, Risk BA, Robyr D, Ruan XA, Sammeth M, Sandhu KS, Schaeffer L, See LH, Shahab A, Skancke J, Suzuki AM, Takahashi H, Tilgner H, Trout D, Walters N, Wang HE, Wrobel J, Yu YB, Hayashizaki Y, Harrow J, Gerstein M, Hubbard TJ, Reymond A, Antonarakis SE, Hannon GJ, Giddings MC, Ruan YJ, Wold B, Carninci P, Guigo R, Gingeras TR, Rosenbloom KR, Sloan CA, Learned K, Malladi VS, Wong MC, Barber G, Cline MS, Dreszer TR, Heitner SG, Karolchik D, Kent WJ, Kirkup VM, Meyer LR, Long JC, Maddren M, Raney BJ, Furey TS, Song LY, Grasfeder LL, Giresi PG, Lee BK, Battenhouse A, Sheffield NC, Simon JM, Showers KA, Safi A, London D, Bhinge AA, Shestak C, Schaner MR, Kim SK, Zhang ZZZ, Mieczkowski PA, Mieczkowska JO, Liu Z, McDaniell RM, Ni YY, Rashid NU, Kim MJ, Adar S, Zhang ZC, Wang TY, Winter D, Keefe D, Birney E, Iyer VR, Lieb JD, Crawford GE, Li GL, Sandhu KS, Zheng MZ, Wang P, Luo OJ, Shahab A, Fullwood MJ, Ruan XA, Ruan YJ, Myers RM, Pauli F, Williams BA, Gertz J, Marinov GK, Reddy TE, Vielmetter J, Partridge EC, Trout D, Varley KE, Gasper C, Bansal A, Pepke S, Jain P, Amrhein H, Bowling KM, Anaya M, Cross MK, King B, Muratet MA, Antoshechkin I, Newberry KM, Mccue K, Nesmith AS, Fisher-Aylor KI, Pusey B, DeSalvo G, Parker SL, Balasubramanian S, Davis NS, Meadows SK, Eggleston T, Gunter C, Newberry JS, Levy SE, Absher DM, Mortazavi A, Wong WH, Wold B, Blow MJ, Visel A, Pennachio LA, Elnitski L, Margulies EH, Parker SCJ, Petrykowska HM, Abyzov A, Aken B, Barrell D, Barson G, Berry A, Bignell A, Boychenko V, Bussotti G, Chrast J, Davidson C, Derrien T, Despacio-Reyes G, Diekhans M, Ezkurdia I, Frankish A, Gilbert J, Gonzalez JM, Griffiths E, Harte R, Hendrix DA, Howald C, Hunt T, Jungreis I, Kay M, Khurana E, Kokocinski F, Leng J, Lin MF, Loveland J, Lu Z, Manthravadi D, Mariotti M, Mudge J, Mukherjee G, Notredame C, Pei BK, Rodriguez JM, Saunders G, Sboner A, Searle S, Sisu C, Snow C, Steward C, Tanzer A, Tapanari E, Tress ML, van Baren MJ, Walters N, Washietl S, Wilming L, Zadissa A, Zhang ZD, Brent M, Haussler D, Kellis M, Valencia A, Gerstein M, Reymond A, Guigo R, Harrow J, Hubbard TJ, Landt SG, Frietze S, Abyzov A, Addleman N, Alexander RP, Auerbach RK, Balasubramanian S, Bettinger K, Bhardwaj N, Boyle AP, Cao AR, Cayting P, Charos A, Cheng Y, Cheng C, Eastman C, Euskirchen G, Fleming JD, Grubert F, Habegger L, Hariharan M, Harmanci A, Iyengar S, Jin VX, Karczewski KJ, Kasowski M, Lacroute P, Lam H, Lamarre-Vincent N, Leng J, Lian J, Lindahl-Allen M, Min RQ, Miotto B, Monahan H, Moqtaderi Z, Mu XMJ, O'Geen H, Ouyang ZQ, Patacsil D, Pei BK, Raha D, Ramirez L, Reed B, Rozowsky J, Sboner A, Shi MY, Sisu C, Slifer T, Witt H, Wu LF, Xu XQ, Yan KK, Yang XQ, Yip KY, Zhang ZD, Struhl K, Weissman SM, Gerstein M, Farnham PJ, Snyder M, Tenenbaum SA, Penalva LO, Doyle F, Karmakar S, Landt SG, Bhanvadia RR, Choudhury A, Domanus M, Ma LJ, Moran J, Patacsil D,

Slifer T, Victorsen A, Yang XQ, Snyder M, White KP, Auer T, Centanin L, Eichenlaub M, Gruhl F, Heermann S, Hoeckendorf B, Inoue D, Kellner T, Kirchmaier S, Mueller C, Reinhardt R, Schertel L, Schneider S, Sinn R, Wittbrodt B, Wittbrodt J, Weng ZP, Whitfield TW, Wang J, Collins PJ, Aldred SF, Trinklein ND, Partridge EC, Myers RM, Dekker J, Jain G, Lajoie BR, Sanyal A, Balasundaram G, Bates DL, Byron R, Canfield TK, Diegel MJ, Dunn D, Ebersol AK, Frum T, Garg K, Gist E, Hansen RS, Boatman L, Haugen E, Humbert R, Jain G, Johnson AK, Johnson EM, Kutyavin TV, Lajoie BR, Lee K, Lotakis D, Maurano MT, Neph SJ, Neri FV, Nguyen ED, Qu HZ, Reynolds AP, Roach V, Rynes E, Sabo P, Sanchez ME, Sandstrom RS, Sanyal A, Shafer AO, Stergachis AB, Thomas S, Thurman RE, Vernot B, Vierstra J, Vong S, Wang H, Weaver MA, Yan YQ, Zhang MH, Akey JM, Bender M, Dorschner MO, Groudine M, MacCoss MJ, Navas P, Stamatoyannopoulos G, Kaul R, Dekker J, Stamatoyannopoulos JA, Dunham I, Beal K, Brazma A, Flicek P, Herrero J, Johnson N, Keefe D, Lukk M, Luscombe NM, Sobral D, Vaquerizas JM, Wilder SP, Batzoglou S, Sidow A, Hussami N, Kyriazopoulou-Panagiotopoulou S, Libbrecht MW, Schaub MA, Kundaje A, Hardison RC, Miller W, Giardine B, Harris RS, Wu W, Bickel PJ, Banfai B, Boley NP, Brown JB, Huang HY, Li QH, Li JJ, Noble WS, Bilmes JA, Buske OJ, Hoffman MM, Sahu AD, Kharchenko PV, Park PJ, Baker D, Taylor J, Weng ZP, Iyer S, Dong XJ, Greven M, Lin XY, Wang J, Xi HLS, Zhuang JL, Gerstein M, Alexander RP, Balasubramanian S, Cheng C, Harmanci A, Lochovsky L, Min R, Mu XMJ, Rozowsky J, Yan KK, Yip KY, Birney E, Consortium EP. An integrated encyclopedia of DNA elements in the human genome. Nature. 2012; 489:57–74. [PubMed: 22955616]

Dymacek J, Snyder-Talkington BN, Porter DW, Wolfarth MG, Castranova V, Qian Y, Guo NL. mRNA and miRNA regulatory networks reflective of multi-walled carbon nanotube-induced lung inflammatory and fibrotic pathologies in mice. Under Review. 2014

FDA US. Adjuvant pazopanib in stage I NSCLC. ClinicalTrials.gov. 2008

FDA US. A double-blind, placebo-controlled, randomized study of the efficacy (Gleevec imatinib mesylate) in patients with idiopathic pulmonary fibrosis. ClincalTrials.gov. 2013

Ferte C, Trister AD, Huang E, Bot BM, Guinney J, Commo F, Sieberts S, Andre F, Besse B, Soria JC, Friend SH. Impact of bioinformatic procedures in the development and translation of high-throughput molecular classifiers in oncology. Clin Cancer Res. 2013; 19:4315–4325. [PubMed: 23780890]

Ganepola GA, Nizin J, Rutledge JR, Chang DH. Use of blood-based biomarkers for early diagnosis and surveillance of colorectal cancer. World J Gastrointest Oncol. 2014; 6:83–97. [PubMed: 24734154]

Garofalo M, Croce CM. microRNAs: Master regulators as potential therapeutics in cancer. Annu Rev Pharmacol Toxicol. 2011; 51:25–43. [PubMed: 20809797]

Gressner AM, Weiskirchen R, Breitkopf K, Dooley S. Roles of TGF-beta in hepatic fibrosis. Front Biosci. 2002; 7:d793–807. [PubMed: 11897555]

Guo NL, Wan YW, Denvir J, Porter DW, Pacurari M, Wolfarth MG, Castranova V, Qian Y. Multiwalled carbon nanotube-induced gene signatures in the mouse lung: potential predictive value for human lung cancer risk and prognosis. J Toxicol Environ Health A. 2012; 75:1129–1153. [PubMed: 22891886]

Hanada T, Yoshimura A. Regulation of cytokine signaling and inflammation. Cytokine Growth Factor Rev. 2002; 13:413–421. [PubMed: 12220554]

Hayashita Y, Osada H, Tatematsu Y, Yamada H, Yanagisawa K, Tomida S, Yatabe Y, Kawahara K, Sekido Y, Takahashi T. A polycistronic microRNA cluster, miR-17-92, is overexpressed in human lung cancers and enhances cell proliferation. Cancer Res. 2005; 65:9628–9632. [PubMed: 16266980]

Hussain S, Sangtian S, Anderson SM, Snyder RJ, Marshburn JD, Rice AB, Bonner JC, Garantziotis S. Inflammasome activation in airway epithelial cells after multi-walled carbon nanotube exposure mediates a profibrotic response in lung fibroblasts. Part Fibre Toxicol. 2014; 11:28. [PubMed: 24915862]

Hwang HW, Mendell JT. MicroRNAs in cell proliferation, cell death, and tumorigenesis. Br J Cancer. 2007; 96:R40–44. Suppl. [PubMed: 17393584]

Iijima S. Helical microtubules of graphitic carbon. Nature. 1991; 354:56–58.

Imielinski M, Berger AH, Hammerman PS, Hernandez B, Pugh TJ, Hodis E, Cho J, Suh J, Capelletti M, Sivachenko A, Sougnez C, Auclair D, Lawrence MS, Stojanov P, Cibulskis K, Choi K, de Waal L, Sharifnia T, Brooks A, Greulich H, Banerji S, Zander T, Seidel D, Leenders F, Ansen S, Ludwig C, Engel-Riedel W, Stoelben E, Wolf J, Goparju C, Thompson K, Winckler W, Kwiatkowski D, Johnson BE, Janne PA, Miller VA, Pao W, Travis WD, Pass HI, Gabriel SB, Lander ES, Thomas RK, Garraway LA, Getz G, Meyerson M. Mapping the hallmarks of lung adenocarcinoma with massively parallel sequencing. Cell. 2012; 150:1107–1120. [PubMed: 22980975]

Irizarry RA, Hobbs B, Collin F, Beazer-Barclay YD, Antonellis KJ, Scherf U, Speed TP. Exploration, normalization, and summaries of high density oligonucleotide array probe level data. Biostatistics. 2003; 4:249–264. [PubMed: 12925520]

Jouan V, Canron X, Alemany M, Caen JP, Quentin G, Plouet J, Bikfalvi A. Inhibition of in vitro angiogenesis by platelet factor-4-derived peptides and mechanism of action. Blood. 1999; 94:984–993. [PubMed: 10419890]

Junk DJ, Bryson BL, Jackson MW. HiJAK'd signaling; the STAT3 paradox in senescence and cancer progression. Cancers (Basel). 2014; 6:741–755. [PubMed: 24675570]

Kang R, Loux T, Tang D, Schapiro NE, Vernon P, Livesey KM, Krasinskas A, Lotze MT, Zeh HJ 3rd. The expression of the receptor for advanced glycation endproducts (RAGE) is permissive for early pancreatic neoplasia. Proc Natl Acad Sci U S A. 2012; 109:7031–7036. [PubMed: 22509024]

Kim YA, Hayashi T, Endo M, Kaburagi Y, Tsukada T, Shan J, Osato K, Tsuruoka S. Synthesis and structural characterization of thin multi-walled carbon nanotubes with a partially facetted cross section by a floating reactant method. Carbon. 2005; 43:2243–2250.

Korpelainen EI, Karkkainen M, Gunji Y, Vikkula M, Alitalo K. Endothelial receptor tyrosine kinases activate the STAT signaling pathway: mutant Tie-2 causing venous malformations signals a distinct STAT activation response. Oncogene. 1999; 18:1–8. [PubMed: 9926914]

Lee RC, Feinbaum RL, Ambros V. The C. elegans heterochronic gene lin-4 encodes small RNAs with antisense complementarity to lin-14. Cell. 1993; 75:843–854. [PubMed: 8252621]

Lee T, Park JY, Lee HY, Cho YJ, Yoon HI, Lee JH, Jheon S, Lee CT, Park JS. Lung cancer in patients with idiopathic pulmonary fibrosis: Clinical characteristics and impact on survival. Respir Med. 2014

Ley B, Brown KK, Collard HR. Molecular Biomarkers in Idiopathic Pulmonary Fibrosis. Am J Physiol Lung Cell Mol Physiol. 2014

Ley B, Collard HR, King TE Jr. Clinical course and prediction of survival in idiopathic pulmonary fibrosis. Am J Respir Crit Care Med. 2011; 183:431–440. [PubMed: 20935110]

Lingle WL, Barrett SL, Negron VC, D'Assoro AB, Boeneman K, Liu W, Whitehead CM, Reynolds C, Salisbury JL. Centrosome amplification drives chromosomal instability in breast tumor development. Proc Natl Acad Sci U S A. 2002; 99:1978–1983. [PubMed: 11830638]

Liu GX, Li YQ, Huang XR, Wei L, Chen HY, Shi YJ, Heuchel RL, Lan HY. Disruption of Smad7 promotes ANG II-mediated renal inflammation and fibrosis via Sp1-TGF-beta/Smad3-NFκB-dependent mechanisms in mice. PLoS One. 2013; 8:e53573. [PubMed: 23301086]

Malkinson AM, Koski KM, Evans WA, Festing MF. Butylated hydroxytoluene exposure is necessary to induce lung tumors in BALB mice treated with 3-methylcholanthrene. Cancer Res. 1997; 57:2832–2834. [PubMed: 9230183]

Marone PA, Hall WC, Hayes AW. Reassessing the two-year rodent carcinogenicity bioassay: a review of the applicability to human risk and current perspectives. Regul Toxicol Pharmacol. 2014; 68:108–118. [PubMed: 24287155]

McKinney W, Chen B, Frazer D. Computer controlled multi-walled carbon nanotube inhalation exposure system. Inhal Toxicol. 2009; 21:1053–1061. [PubMed: 19555230]

Mercer RR, Scabilloni JF, Hubbs AF, Battelli LA, McKinney W, Friend S, Wolfarth MG, Andrew M, Castranova V, Porter DW. Distribution and fibrotic response following inhalation exposure to multi-walled carbon nanotubes. Part Fibre Toxicol. 2013a; 10:33. [PubMed: 23895460]

Mercer RR, Scabilloni JF, Hubbs AF, Wang L, Battelli LA, McKinney W, Castranova V, Porter DW. Extrapulmonary transport of MWCNT following inhalation exposure. Part Fibre Toxicol. 2013b; 10:38. [PubMed: 23927530]

Mohri T, Fujio Y, Maeda M, Ito T, Iwakura T, Oshima Y, Uozumi Y, Segawa M, Yamamoto H, Kishimoto T, Azuma J. Leukemia inhibitory factor induces endothelial differentiation in cardiac stem cells. J Biol Chem. 2006; 281:6442–6447. [PubMed: 16407199]

Nagai H, Okazaki Y, Chew SH, Misawa N, Yamashita Y, Akatsuka S, Ishihara T, Yamashita K, Yoshikawa Y, Yasui H, Jiang L, Ohara H, Takahashi T, Ichihara G, Kostarelos K, Miyata Y, Shinohara H, Toyokuni S. Diameter and rigidity of multiwalled carbon nanotubes are critical factors in mesothelial injury and carcinogenesis. Proc Natl Acad Sci U S A. 2011; 108:E1330–1338. [PubMed: 22084097]

Nakao A, Fujii M, Matsumura R, Kumano K, Saito Y, Miyazono K, Iwamoto I. Transient gene transfer and expression of Smad7 prevents bleomycin-induced lung fibrosis in mice. J Clin Invest. 1999; 104:5–11. [PubMed: 10393693]

Nawroth R, Poell G, Ranft A, Kloep S, Samulowitz U, Fachinger G, Golding M, Shima DT, Deutsch U, Vestweber D. VE-PTP and VE-cadherin ectodomains interact to facilitate regulation of phosphorylation and cell contacts. EMBO J. 2002; 21:4885–4895. [PubMed: 12234928]

NCI NCI. Celecoxib and docetaxel or pemetrexed in treating patients with advanced recurrent non-small cell lung cancer. ClinicalTrials.gov. 2007

Oak SR, Murray L, Herath A, Sleeman M, Anderson I, Joshi AD, Coelho AL, Flaherty KR, Toews GB, Knight D, Martinez FJ, Hogaboam CM. A micro RNA processing defect in rapidly progressing idiopathic pulmonary fibrosis. PLoS One. 2011; 6:e21253. [PubMed: 21712985]

Oritani K, Medina KL, Tomiyama Y, Ishikawa J, Okajima Y, Ogawa M, Yokota T, Aoyama K, Takahashi I, Kincade PW, Matsuzawa Y. Limitin: An interferon-like cytokine that preferentially influences B-lymphocyte precursors. Nat Med. 2000; 6:659–666. [PubMed: 10835682]

Pandiri A. Comparative pathobiology of environmentally induced lung cancers in humans and rodents. Toxicol Pathol. 2014

Pandit KV, Corcoran D, Yousef H, Yarlagadda M, Tzouvelekis A, Gibson KF, Konishi K, Yousem SA, Singh M, Handley D, Richards T, Selman M, Watkins SC, Pardo A, Ben-Yehudah A, Bouros D, Eickelberg O, Ray P, Benos PV, Kaminski N. Inhibition and role of let-7d in idiopathic pulmonary fibrosis. Am J Respir Crit Care Med. 2010; 182:220–229. [PubMed: 20395557]

Pandit KV, Milosevic J, Kaminski N. MicroRNAs in idiopathic pulmonary fibrosis. Transl Res. 2011; 157:191–199. [PubMed: 21420029]

Pitot HC. Multistage carcinogenesis--genetic and epigenetic mechanisms in relation to cancer prevention. Cancer Detect Prev. 1993; 17:567–573. [PubMed: 8275509]

Piu F, Magnani M, Ader ME. Dissection of the cytoplasmic domains of cytokine receptors involved in STAT and Ras dependent proliferation. Oncogene. 2002; 21:3579–3591. [PubMed: 12032860]

Porter DW, Hubbs AF, Chen BT, McKinney W, Mercer RR, Wolfarth MG, Battelli L, Wu N, Sriram K, Leonard S, Andrew M, Willard P, Tsuruoka S, Endo M, Tsukada T, Munekane F, Frazer DG, Castranova V. Acute pulmonary dose-responses to inhaled multi-walled carbon nanotubes. Nanotoxicology. 2013; 7:1179–1194. [PubMed: 22881873]

Porter DW, Hubbs AF, Mercer RR, Wu N, Wolfarth MG, Sriram K, Leonard S, Battelli L, Schwegler-Berry D, Friend S, Andrew M, Chen BT, Tsuruoka S, Endo M, Castranova V. Mouse pulmonary dose- and time course-responses induced by exposure to multi-walled carbon nanotubes. Toxicology. 2010; 269:136–147. [PubMed: 19857541]

Posselt G, Schwarz H, Duschl A, Horejs-Hoeck J. Suppressor of cytokine signaling 2 is a feedback inhibitor of TLR-induced activation in human monocyte-derived dendritic cells. J Immunol. 2011; 187:2875–2884. [PubMed: 21844389]

Puissegur MP, Mazure NM, Bertero T, Pradelli L, Grosso S, Robbe-Sermesant K, Maurin T, Lebrigand K, Cardinaud B, Hofman V, Fourre S, Magnone V, Ricci JE, Pouyssegur J, Gounon P, Hofman P, Barbry P, Mari B. miR-210 is overexpressed in late stages of lung cancer and mediates mitochondrial alterations associated with modulation of HIF-1 activity. Cell Death Differ. 2011; 18:465–478. [PubMed: 20885442]

Raponi M, Dossey L, Jatkoe T, Wu X, Chen G, Fan H, Beer DG. MicroRNA classifiers for predicting prognosis of squamous cell lung cancer. Cancer Res. 2009; 69:5776–5783. [PubMed: 19584273]

Redova M, Sana J, Slaby O. Circulating miRNAs as new blood-based biomarkers for solid cancers. Future Oncol. 2013; 9:387–402. [PubMed: 23469974]

Redova M, Svoboda M, Slaby O. MicroRNAs and their target gene networks in renal cell carcinoma. Biochem Biophys Res Commun. 2011; 405:153–156. [PubMed: 21232526]

Rittinghausen S, Hackbarth A, Creutzenberg O, Ernst H, Heinrich U, Leonhardt A, Schaudien D. The carcinogenic effect of various multi-walled carbon nanotubes (MWCNTs) after intraperitoneal injection in rats. Part Fibre Toxicol. 2014; 11:59. [PubMed: 25410479]

Russell WM. The development of the three Rs concept. Altern Lab Anim. 1995; 23:298–304. [PubMed: 11656565]

Sargent LM, Porter DW, Staska LM, Hubbs AF, Lowry DT, Battelli L, Siegrist KJ, Kashon ML, Mercer RR, Bauer AK, Chen BT, Salisbury JL, Frazer D, McKinney W, Andrew M, Tsuruoka S, Endo M, Fluharty KL, Castranova V, Reynolds SH. Promotion of lung adenocarcinoma following inhalation exposure to multi-walled carbon nanotubes. Part Fibre Toxicol. 2014; 11:3. [PubMed: 24405760]

Savci-Heijink CD, Kosari F, Aubry MC, Caron BL, Sun Z, Yang P, Vasmatzis G. The role of desmoglein-3 in the diagnosis of squamous cell carcinoma of the lung. Am J Pathol. 2009; 174:1629–1637. [PubMed: 19342368]

Sawant DV, Sehra S, Nguyen ET, Jadhav R, Englert K, Shinnakasu R, Hangoc G, Broxmeyer HE, Nakayama T, Perumal NB, Kaplan MH, Dent AL. Bcl6 controls the Th2 inflammatory activity of regulatory T cells by repressing Gata3 function. J Immunol. 2012; 189:4759–4769. [PubMed: 23053511]

Schaaij-Visser TB, de Wit M, Lam SW, Jimenez CR. The cancer secretome, current status and opportunities in the lung, breast and colorectal cancer context. Biochim Biophys Acta. 2013; 1834:2242–2258. [PubMed: 23376433]

Seike M, Goto A, Okano T, Bowman ED, Schetter AJ, Horikawa I, Mathe EA, Jen J, Yang P, Sugimura H, Gemma A, Kudoh S, Croce CM, Harris CC. MiR-21 is an EGFR-regulated anti-apoptotic factor in lung cancer in never-smokers. Proc Natl Acad Sci U S A. 2009; 106:12085–12090. [PubMed: 19597153]

Selbach M, Schwanhausser B, Thierfelder N, Fang Z, Khanin R, Rajewsky N. Widespread changes in protein synthesis induced by microRNAs. Nature. 2008; 455:58–63. [PubMed: 18668040]

Siegrist KJ, Reynolds SH, Kashon ML, Lowry DT, Dong C, Hubbs AF, Young SH, Salisbury JL, Porter DW, Benkovic SA, McCawley M, Keane MJ, Mastovich JT, Bunker KL, Cena LG, Sparrow MC, Sturgeon JL, Dinu CZ, Sargent LM. Genotoxicity of multi-walled carbon nanotubes at occupationally relevant doses. Part Fibre Toxicol. 2014; 11:6. [PubMed: 24479647]

Snyder-Talkington BN, Dong C, Zhao X, Dymacek J, Porter DW, Wolfarth MG, Castranova V, Qian Y, Guo NL. Multi-walled carbon nanotube-induced gene expression in vitro: Concordance with in vivo studies. Toxicology. 2015; 328:66–74. [PubMed: 25511174]

Snyder-Talkington BN, Dymacek J, Porter DW, Wolfarth MG, Mercer RR, Pacurari M, Denvir J, Castranova V, Qian Y, Guo NL. System-based identification of toxicity pathways associated with multi-walled carbon nanotube-induced pathological responses. Toxicol Appl Pharmacol. 2013a; 272:476–489. [PubMed: 23845593]

Snyder-Talkington BN, Pacurari M, Dong C, Leonard SS, Schwegler-Berry D, Castranova V, Qian Y, Guo NL. Systematic analysis of multiwalled carbon nanotube-induced cellular signaling and gene expression in human small airway epithelial cells. Toxicol Sci. 2013b; 133:79–89. [PubMed: 23377615]

Snyder-Talkington BN, Schwegler-Berry D, Castranova V, Qian Y, Guo NL. Multi-walled carbon nanotubes induce human microvascular endothelial cellular effects in an alveolar-capillary co-culture with small airway epithelial cells. Part Fibre Toxicol. 2013c; 10:35. [PubMed: 23903001]

Strieter RM. What differentiates normal lung repair and fibrosis? Inflammation, resolution of repair, and fibrosis. Proc Am Thorac Soc. 2008; 5:305–310. [PubMed: 18403324]

Tani-ichi S, Shimba A, Wagatsuma K, Miyachi H, Kitano S, Imai K, Hara T, Ikuta K. Interleukin-7 receptor controls development and maturation of late stages of thymocyte subpopulations. Proc Natl Acad Sci U S A. 2013; 110:612–617. [PubMed: 23267098]

Vancheri C, Failla M, Crimi N, Raghu G. Idiopathic pulmonary fibrosis: a disease with similarities and links to cancer biology. Eur Respir J. 2010; 35:496–504. [PubMed: 20190329]

Wang Q, Li DC, Li ZF, Liu CX, Xiao YM, Zhang B, Li XD, Zhao J, Chen LP, Xing XM, Tang SF, Lin YC, Lai YD, Yang P, Zeng JL, Xiao Q, Zeng XW, Lin ZN, Zhuang ZX, Zhuang SM, Chen W. Upregulation of miR-27a contributes to the malignant transformation of human bronchial epithelial cells induced by SV40 small T antigen. Oncogene. 2011; 30:3875–3886. [PubMed: 21460851]

Wei F, Zaprazna K, Wang J, Atchison ML. PU.1 can recruit BCL6 to DNA to repress gene expression in germinal center B cells. Mol Cell Biol. 2009; 29:4612–4622. [PubMed: 19564417]

Wu X, Chen L, Wang X. Network biomarkers, interaction networks and dynamical network biomarkers in respiratory diseases. Clin Transl Med. 2014; 3:16. [PubMed: 24995123]

Xiong Y, Huo Y, Chen C, Zeng H, Lu X, Wei C, Ruan C, Zhang X, Hu Z, Shibuya M, Luo J. Vascular endothelial growth factor (VEGF) receptor-2 tyrosine 1175 signaling controls VEGF-induced von Willebrand factor release from endothelial cells via phospholipase C-gamma 1- and protein kinase A-dependent pathways. J Biol Chem. 2009; 284:23217–23224. [PubMed: 19570985]

Yanagita M, Arai H, Nakano T, Ohashi K, Mizuno K, Fukatsu A, Doi T, Kita T. Gas6 induces mesangial cell proliferation via latent transcription factor STAT3. J Biol Chem. 2001; 276:42364–42369. [PubMed: 11546821]

Zhou P, Wang Z, Yuan X, Zhou C, Liu L, Wan X, Zhang F, Ding X, Wang C, Xiong S, Wang Z, Yuan J, Li Q, Zhang Y. Mixed lineage leukemia 5 (MLL5) protein regulates cell cycle progression and E2F1-responsive gene expression via association with host cell factor-1 (HCF-1). J Biol Chem. 2013; 288:17532–17543. [PubMed: 23629655]
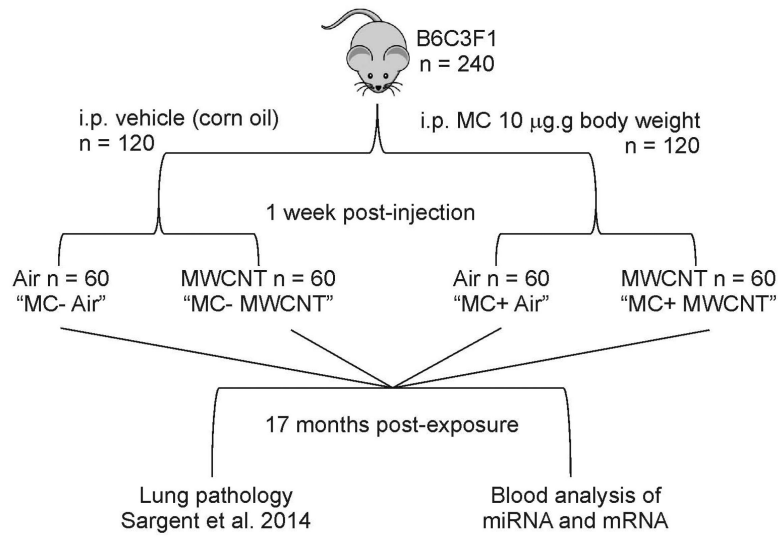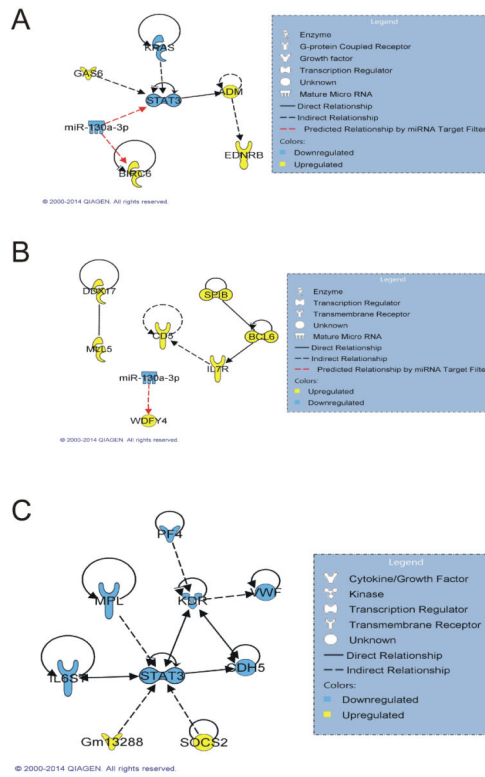
Figure 1.
Schematic of mouse exposure groups and analysis.
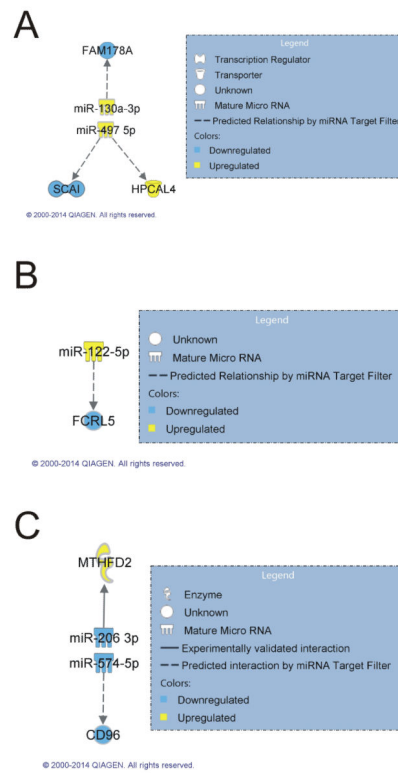
Figure 2.
Regulatory networks between mRNAs and miRNAs. Regulatory networks between significant mRNAs (FDR 10%, FC>1.5) and miRNAs (FDR 10%, FC >1.2) in the (A) MCA bronchiolo-alveolar adenoma, (B) MWCNT hyperplasia, and (C) MCA+MWCNT fibrosis categories were determined by using an IPA miRNA Target Filter.
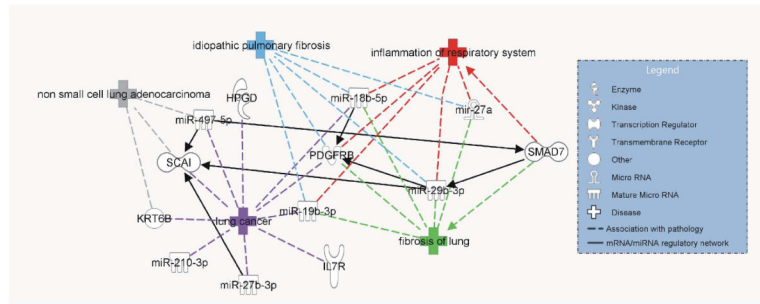
Figure 3.
Association of mRNAs and miRNAs with IPA literature-based lung abnormalities. All significant mRNAs (FDR 10%, FC >1.5) and miRNAs (FDR 10%, FC >1.2) were input into IPA, and an IPA disease and functions overlay was used to determine their association with the IPA diseases idiopathic pulmonary fibrosis, inflammation of respiratory system, fibrosis of lung, lung cancer, and non-small cell lung adenocarcinoma

Figure 4.
Regulatory networks in bronchiolo-alveolar adenocarcinoma versus adenoma. Regulatory networks between significant mRNAs (FDR 10%, FC >1.5) and miRNAs (FDR 10%, FC >1.2) involved in bronchiolo-alveolar adenocarcinoma versus adenoma in the (A) Air, (B) MCA, and (C) MCA+MWCNT groups were determined by using an IPA miRNA Target Filter.

Table 1

Number of mice and blood samples in each pathology group.

	MC– Air	MC+ Air	MC– MWCNT	MC+ MWCNT
Total number of mice in each pathology category	60	60	55	55
Focal alveolar hyperplasia	7 (12%)	8 (13%)	14 (25%)	30 (55%)
Bronchiolo-alveolar hyperplasia	1 (2%)	9 (15%)	45 (82%)	37 (67%)
Fibrosis	1 (2%)	5 (8%)	4 (7%)	10 (18%)
Bronchiolo-alveolar adenoma	6 (10%)	20 (33%)	9 (16%)	37 (67%)
Bronchiolo-alveolar adenocarcinoma	7 (12%)	13 (22%)	7 (13%)	33 (60%)
Total number of blood samples with sufficient mRNA in each category	**45**	**42**	**40**	**33**
Hyperplasia[*]	7 (16%)	13 (31%)	33 (83%)	27 (82%)
Fibrosis	3 (7%)	8 (19%)	4 (10%)	8 (24%)
Bronchiolo-alveolar adenoma	5 (11%)	17 (40%)	8 (20%)	24 (73%)
Bronchiolo-alveolar adenocarcinoma	6 (13%)	9 (21%)	7 (18%)	20 (61%)
Total number of blood samples with sufficient miRNA in each category	**43**	**36**	**37**	**30**
Hyperplasia[*]	7 (16%)	11 (31%)	30 (81%)	25 (83%)
Fibrosis	3 (7%)	7 (19%)	4 (11%)	7 (23%)
Bronchiolo-alveolar adenoma	4 (9%)	15 (42%)	8 (22%)	22 (73%)
Bronchiolo-alveolar adenocarcinoma	6 (14%)	9 (25%)	5 (14%)	18 (60%)

Values are shown as n (%) of the total number of mice or blood samples analyzed in that group. Mice with multiple instances of a single pathology in different lung lobes were only counted once.

[*] Hyperplasia refers to both focal alveolar and bronchiolo-alveolar hyperplasia. Reasons for having fewer blood samples than the total number of mice in a treatment category included insufficient blood draws, insufficient mRNA or miRNA quantity or quality for analysis, and early death of a mouse that prohibited whole blood collection.

Table 2

mRNA and miRNA in MC– Air mice developing lung pathology (pathology control mice) significantly up-or down-regulated when compared to MC– Air mice with normal lung tissue (normal control mice).

	mRNA	miRNA
Hyperplasia		**Up-regulated:** miR-340-5p
Fibrosis	**Up-regulated:** 17200163 **Down-regulated:** Rhox3h	**Up-regulated:** miR-200c-3p, miR-26b-5p, miR-702-5p, miR-30a-3p, miR-140-5p, miR-146a-5p, miR-151-5p, miR-27b-3p, miR-425-5p, miR-192-5p, miR-194-5p **Down-regulated:** miR-345-5p, miR-145a-5p, miR-29c-3p, miR425-3p, miR-6240, miR-122-5p, miR-10a-5p, miR-326-3p, miR-339-5p, miR-378a-5p
Bronchiolo-alveolar Adenoma	**Up-regulated:** 17200713, 17460573, A230057D06Rik, Rhox2g	**Up-regulated:** miR-466c-5p **Down-regulated:** miR-690, miR-29b-3p, miR-497-5p, miR-425-3p, miR-500-3p, miR-345-5p, miR-144-3p, miR-5112
Bronchiolo-alveolar Adenocarcinoma	**Up-regulated:** 17225809, 17313575, 17448801 **Down-regulated:** cc119	**Down-regulated:** miR-345-5p, miR-144-3p, miR-130a-3p, miR-19a-3p, miR-29b-3p, miR-19b-3p, miR-362-5p, miR-497-5p

Table 3

Significant mRNAs and miRNAs in each treatment group versus normal control mice, FC >1.5, FDR <10%, bold underline indicates a potential genetic factor

	mRNA	miRNA
MC+ Air		
Hyperplasia	**Upregulated:** iqcg, 17202511, siglich, 9830166K06Rik **Downregulated:** 1720663	**Upregulated:** miR-29b-3p, miR-15a-3p, miR-362-3p, miR-5112, miR-5131, miR-2137
Fibrosis	**Upregulated:** 17209629, 17210565, olfr1062, gm5512, c1, ceacam19 **Downregulated:** uck2, 17203041	**Upregulated:** miR-5131, miR-2137, miR-466c-5p **Downregulated:** miR-6238, miR-32-3p
Bronchiolo-alveolar adenoma	**Upregulated:,** 17210565, scgb2b26, hpcal4, vmn1r65 **Downregulated:** cd3d, 17257054, serpina3f, d10jhu81e, zcchc9, sptssa, fabp4, scai, fam178a	**Upregulated:** <u>**miR-345-5p**</u>, miR-497-5p, miR-130a-3p, miR-15a-3p, miR-5131, miR-2137 **Downregulated:** miR-669c-3p
Bronchiolo-alveolar adenocarcinoma	**Upregulated:** elovl3, hpgd, 17202937, akr1c12, ear2, 17460573 **Downregulated:** fmo3, sp140	
MC– MWCNT		
Hyperplasia	**Upregulated:** 17210565 **Downregulated:** igkv4-91, fcrl5, 17202925, efemp1, gm13139	**Upregulated:** miR-122-5p, miR-497-5p
Fibrosis	**Upregulated:** pdgfrb **Downregulated:** smad7	**Upregulated:** miR-324-5p miR-27a, <u>**miR-27b-3p**</u> **Downregulated:** let-7d-3p, miR-30c-1-3p, miR-3072-5p, miR-5107-5p, miR-341-3p, miR-1892, miR-6370, miR-6368, miR-1249-5p, miR-504-3p, miR-1947-3p
Bronchiolo-alveolar adenoma	**Upregulated:** A630077, j23Rik, myl6b, ighg3 **Downregulated:** 17202925	**Upregulated:** miR-122-5p
Bronchiolo-alveolar adenocarcinoma	**Upregulated:** foxo1, 17210589 **Downregulated:** fcrl5, fcrla, gprl83, 17202023	
MCA+MWCNT		
Hyperplasia	**Upregulated:** gpr114, 01fr984 **Downregulated:** 17205523, sloc1a4, ill8r1, gm6793	**Upregulated:** miR-5112, miR-345-5p **Downregulated:** miR-1957
Fibrosis	**Upregulated:** myh7, mthfd2 **Downregulated:** cd96, tnfrsf23, igh-vj558	**Upregulated:** miR-101b-3p, <u>**miR-29c-3p,**</u> miR-340-5p, miR-18b-5p, **Downregulated:** miR-672-5p, miR-574-5p, miR-206-3p, miR-6348, miR-32-3p, miR-466o-5p, miR-466c-5p, miR-669k-5p
Bronchiolo-alveolar adenoma	**Upregulated:** 17200621, smok2a, krt6a **Downregulated:** 17205967, gm6793, fabp4	**Upregulated:** <u>**miR-345-5p,**</u> <u>**miR-144-3p,**</u> miR-122-5p, miR-19a-3D, <u>**miR-29b-3p,**</u> <u>**miR-19b-3p,**</u> <u>**miR-5112,**</u> miR-5131, miR-15a-3p **Downregulated:** <u>**miR-466c-5p,**</u> miR-5099, miR-5121, miR-1957
Bronchiolo-alveolar adenocarcinoma	**Downregulated:** 17207465, c1qbp, il7r, fcrl5, gpr114, prdm9, sap30bp, krt6a, 17200649, 17202925	**Upregulated:** miR-5112, miR-5131, miR-210-3p, <u>**miR-19b-3p,**</u> <u>**miR-345-5p**</u> **Downregulated:** miR-466c-5p

Table 4

Significant mRNAs and miRNAs in each treatment group compared between adenoma and adenocarcinoma outcomes, FC >1.5, FDR <10%, bold underline indicates a potential genetic factor

	MC– Air	Mc+ MCA	MC– MWCNT	MCA+ MWCNT
mRNA	**Upregulated:**, zfp942, zfp709, thoc7, robol, pdcd4, gas6, ednrb, cldn3, birc6, adm, hla-a, 2410017I17Rik, 17415391, 17474676 **Downregulated:** stats, selp, rrml, rpsl9bpl, mfl66, pfkp, olfr750, kras, clec9a, A830052DllRik, 17203463, 17482738	**Upregulated:** usp9x, ptger4, map2kl, kctdl, chd8, spib,wdfy4, bri3bp, mll5, pdzd8, cd5, il7r, rasal3, chdl, slcl5a2, ighm, bcl6, ighg, ddxl7, cd300e, tmeml84b, eif4ebp2, fam105a, ighm **Downregulated:** defb46, snord116, vmnlrl21, vmnlrl80, 4933409K07Rik, 17350691, olfr750, olfr749, gm5458, gm3002, gml0338, gml0413, gm3594, gm 10408, gm906, 17303135	**Upregulated:** topors, pparg, ifit2, sstyl, ckap2, ccdc54, gml3288, sly **Downregulated:** 17209147, gm20759, cacng2, sstr5, kdm3b, bcl10, idua, erp29, loxl3, igk, igkv6-23, vmnlrl29, gm21142, dkk4, clcn3	**Upregulated**: ascl1, olfr46, socs2, ssty1, sly, gm 13288, vwf, bcl10, lmtk2, 17326563, 17206165 **Downregulated:** **stat3,** rin3, 17284562, il6st, c6, myl9, akrla1l, mpl, ccl1 9, abcb4, pf4, chfr, chic2, kdr, A430089I19Rik, hscb, sbnol, gm3139, 0610030E20Rik, ppp4r2, vwf, igkv4-91, sirt2, **rrml,** snordl16, cdh5, cmip, scamp2, bcl2a1a
miRNA	**Upregulated:** miR-25-5p **Downregulated:** miR-130a-3p, miR-6349, miR-6370, miR-467a-5p, miR-374b-5p	**Upregulated:** miR-466g **Downregulated:** miR-425-3p, **miR-130a-3p**, miR-130b-3p, miR-145a-5p, miR-5132-5p, miR-345-5p, miR-211-3p, miR-3090-5p, miR-92a-2-5p,miR-3102-5p	**Upregulated:** miR-6239 **Downregulated:** miR-143-3p, miR-145a-5p, miR-3473a, miR-345-5p, miR199a-l, miR-680-1	**Upregulated:** miR-5119 **Downregulated:** miR-203-3p, miR-126-3p, miR-449a-5p, miR-3102-5p, miR-191